Cumhuriyet Science Journal

e-ISSN: 2587-246X
ISSN: 2587-2680

Cumhuriyet Sci. J., 42(1) (2021) 45-59
http://dx.doi.org/10.17776/csj.826772

Computational study on the structural, electronic, molecular and thermochemical properties of hypothetical [Tp(CO)2Mo≡C-Ph)]2+ and [L(CO)2Mo≡C-Ph)]+ carbyne complexes

Zinet ZAİM , ***Duran KARAKAŞ*** *

Sivas Cumhuriyet University, Science Faculty, Chemistry Department, 58140 SİVAS, TURKEY

Abstract

The structural, electronic, molecular and thermochemical properties of hypothetical [Tp(CO)2Mo≡C-Ph)]2+ (1) [Tp = hydridotris(pyrazolyl) borate] and [L(CO)2Mo≡C-Ph)]+ (2) [L=hydrido 2-phenoxybis(pyrazolyl) borate] carbyne complexes were investigated by quantum chemical calculations. The carbyne complexes were optimized at B3LYP/LANL2DZ/6-31G(d) level. Structural parameters, vibration spectra, electronic spectra and NMR spectra were computationally obtained. Environment geometry of the molybdenum atom was predicted to be distorted octahedral. Mulliken atomic charges, molecular electrostatic potential maps, molecular orbital energy diagrams and frontier orbital contour diagrams were calculated and interpreted to estimate the electronic properties of the complexes. In order to predict the molecular properties of complexes, some electronic structure descriptors were calculated and discussed. The thermal stability of the complexes was investigated. Thermochemical parameters of the complexes were found to increase with increasing temperature. Metal-carbyne bond dissociation energies of complex (1) and complex (2) were calculated as 955 and 912 K, respectively.

Article info

History:
Received: 16.11.2020
Accepted: 12.02.2021

Keywords:
Carbyne complex, Computational research, Spectroscopic analysis, Molecular properties, Thermochemical stability.

1. Introduction

$L_nM{\equiv}C\text{-}R$ type organometallic compounds are known as alkylidyne or carbyne complexes. The ligands in the C-R general formula (R = H, alkyl, aryl, $SiMe_3$, NEt_2, PMe_3, SPh, Cl) are called alkylidyne or carbyne ligands [1] and L ligands are ancillary ligands. Such compounds are used in the synthesis of alkynes and nitriles and act as catalysts in organic reactions [2,3]. Carbyne complexes catalyze alkyne metathesis reactions and form new alkyne compounds. Ancillary ligands have important roles on the catalytic activities of the carbyne complexes and the steric and electronic properties of ancillary ligands are generally considered as important factors to improve the catalytic activity [4-7].

In carbyne complexes, the metal-carbon bond can be considered as a combination of a σ bond and two π bonds. As seen in Fig. 1, sp hybrid orbital on the carbon atom of the carbyne ligand contains a lone electron pair. This lone electron pair is transferred to a suitable orbital on the metal atom and an M-C σ bond is formed. In addition, carbyne carbon has two empty p orbitals. Electrons are transferred from metal to empty p orbitals of the carbyne ligand and two π bonds are formed [8]. As understood from this description, the carbyne ligand is both a σ donor and π receptor. Schematic representation of overlapping orbitals in the formation of σ and π bonds in carbyne complexes is given in Figure 1.

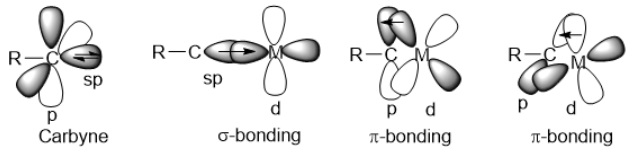

Figure 1. Orbital overlaps in the formation of σ and π bonds in carbyne complexes

Various methods have been used in the synthesis of carbyne complexes. One of them is the Fischer method. The first carbyne complex was synthesized by Fischer and Schubert in 1975 by this method [1]. In this method, when the carbene complex is reacted with Lewis acids of the type BX_3 (X = Cl, Br, I), Lewis acid first attacks the oxygen atom bound to the carbene carbon and the methoxy group is attached to the Lewis acid of the type BX_3. For the first time, $[(CO)_4ClCr{\equiv}C\text{-}Ph]$ carbyne complex was synthesized from the

*Corresponding author. e-*mail address: dkarakas@cumhuriyet.edu.tr*
 ©2021 Faculty of Science, Sivas Cumhuriyet University

reactions of carbene complexes with Lewis acids [9]. The structure of the complex was examined by X-ray crystallography. The other method used in synthesizing the carbyne complexes is the Mayr procedure [10]. In this method, the carbene complexes are reacted with oxalyl chloride in a solvent of dichloromethane at low temperatures to form a halide-containing carbyne intermediate. Carbyne complex is prepared by adding a strong multi-dental ligand on this intermediate at low temperatures. Stone and colleagues used the Mayr procedure to prepare $Cp(CO)_2M{\equiv}C$-R/Ar and $Tp(CO)_2W{\equiv}C$-Tol type carbyne complexes. Where Cp=cyclopentadienyl, Tp=hydridotris(pyrazolyl)borate and Tol=p-tolyl [9,11,12]. In addition, new Fischer type tungsten carbyne complexes such as $L(CO)_2W{\equiv}C$-R/Ar were synthesized by A. Sarkar at al. using the Mayr method [13]. Here L is a tridentate and -1 charged ligand. In this study, it was found that the synthesized complexes were thermally stable and did not decompose in long term storage at room temperature.

Although extensive studies have been conducted on other organometallic compounds such as metal carbonyls and carbene complexes, research on carbyne complexes is limited due to the thermal instability of the carbyne complexes. The development of quantum chemical calculation methods and advancement in computer technology made it easier to predict the structural, electronic and molecular characteristic of complexes. In this work, the structural, electronic, molecular and thermochemical properties of hypothetical $[Tp(CO)_2Mo{\equiv}C\text{-}Ph)]^{2+}$ **(1)** and $[L(CO)_2Mo{\equiv}C\text{-}Ph)]^{+}$ **(2)** alkylidyne complexes were investigated by quantum chemical calculations. Where Tp is hydrido tris(pyrazolyl)borate] and L is hydrido 2-phenoxy bis(pyrazolyl)borate. In order to determine the structure of hypothetical complexes, molecular structure parameters, IR, UV-VIS and NMR spectra were computed. Electronic properties were determined by calculating molecular orbital energy diagrams, molecular electrostatic potential maps and electronic charges of atoms. Various molecular structure identifying were calculated to estimate the molecular properties. Thermochemical parameters, total energy (E), enthalpy (H), heat capacity (C_v) and entropy (S) values of the complexes were calculated at 200, 298.15 and 400 K temperatures to predict the complex stability. Correlations were generated which allowed the calculation of thermochemical parameters of complexes at various temperatures.

2. Materials and Methods

Quantum chemical calculations were made on hypothetical $[Tp(CO)_2Mo{\equiv}C\text{-}Ph)]^{2+}$ and $[L(CO)_2Mo{\equiv}C\text{-}Ph)]^{+}$ carbyne complexes. GaussView 5.0.8 program [14] was used for drawing complex structures, preparation of account input files and visualization of the calculation results, Gaussian 09 AS64L-G09 RevD.01 program [15] for the calculations, and ChemDraw Professional 17.0 program for editing the visualized results and saving them as word files. Optimized structure calculations were performed with B3LYP hybrid functional based on density functional theory (DFT) method [16,17]. In the calculations, LANL2DZ/6-31G(d) mixed base set was used [18,19]. The central molybdenum atomic orbitals were represented by the LANL2DZ base set containing the internal potential, the remaining atomic orbitals in the complex were represented by the 6-31G (d) base set. The base set 6-31G(d) is the polarized base set that adds d functions to non-hydrogen atoms. Spin multiplicity of the complexes was taken as singlet and closed shell calculations were made. No negative frequency was calculated as a result of the optimization. This result indicates that the calculated structures are in the ground state.

For the structural analysis, some bond length, bond angles, IR spectrum, UV-VIS spectrum, NMR spectrum of the complexes were calculated. Molecular structural parameters and IR spectrum were obtained from gas phase optimizations. The electronic spectra of the carbyne complexes were calculated at the TD/B3LYP/LANL2DZ/6-31G(d) level and the electronic transitions of the bands in the spectra were investigated. ^{1}H-NMR and ^{13}C-NMR spectra were computed at GIAO/B3LYP/LANL2DZ/6-31G(d) levels and chemical shift values were found according to TMS standard. In order to predict the electronic properties of complexes, Mulliken charges of atoms, electrophilic and nucleophilic regions of complexes and contour diagrams of frontier orbitals were obtained. In order to predict the molecular properties of the complexes, HOMO and LUMO energies were taken from the molecular orbital energy diagrams and some molecular structure descriptors such as ionization energy (I), electron affinity (A), LUMO-HOMO energy gap (ΔE), hardness (η), softness (σ), Mulliken electronegativity (χ), chemical potential (CP), electrophilicity index (ω), static dipole moment (μ) and average linear polarizability (α) were calculated by using eq. (1)-(10) [19,20].

$$I = -E_{HOMO} \quad (1)$$

$$A = -E_{LUMO} \quad (2)$$

$$\Delta E = E_{LUMO} - E_{HOMO} \quad (3)$$

$$\eta = \frac{E_{LUMO} - E_{HOMO}}{2} \quad (4)$$

$$\sigma = \frac{1}{\eta} \quad (5)$$

$$\chi = -\frac{E_{HOMO} + E_{LUMO}}{2} \quad (6)$$

$$\mu_{cp} = -\chi \quad (7)$$

$$\omega = \frac{\mu_{cp}^2}{2\eta} \quad (8)$$

$$\mu = \sqrt{\left(\mu_x^2 + \mu_y^2 + \mu_z^2\right)} \quad (9)$$

$$\alpha = \frac{1}{3}\left(\alpha_{xx} + \alpha_{yy} + \alpha_{zz}\right) \quad (10)$$

Thermochemical parameters which are total energy (E), enthalpy (H), heat capacity (C_v) and entropy (S) were calculated at 200, 298.15 and 400 K temperatures. The temperature dependence of complexes stability was investigated computationally.

3. Results and Discussions

3.1. Structural characterization

Optimized structures of $[Tp(CO)_2Mo{\equiv}C\text{-}Ph)]^{2+}$ and $[L(CO)_2Mo{\equiv}C\text{-}Ph)]^{+}$ carbyne complexes were computed at B3LYP/LANL2DZ/6-31G(d) level in the gas phase under standard conditions (1.00 atm and 298.15 K) and given in Fig. 2 together with atomic labels. Some structure parameters which are obtained from the optimized structures are given in Table 1 and Table 2.

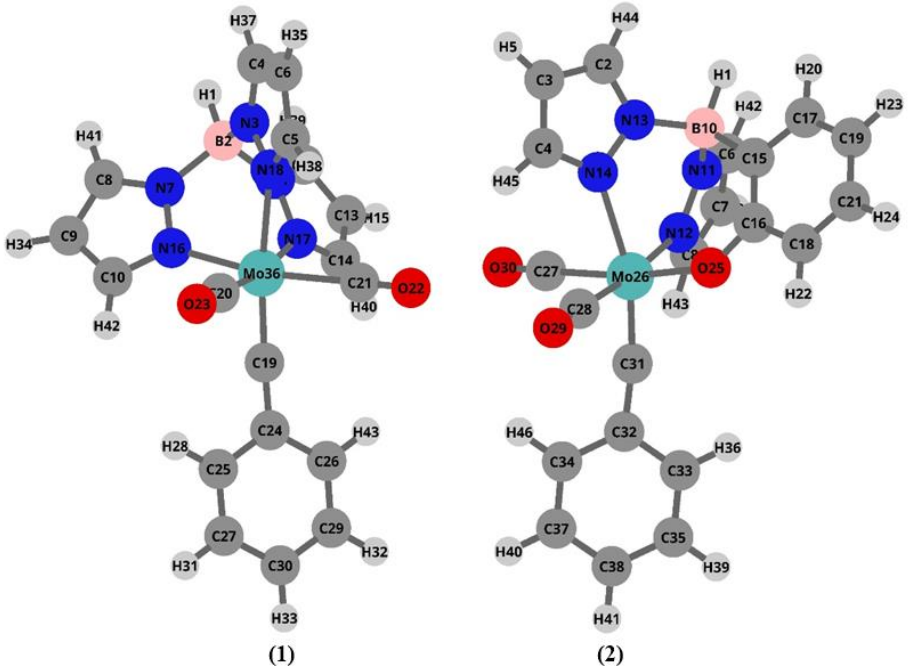

Figure 2. Molecular structure of the $[Tp(CO)_2Mo{\equiv}C\text{-}Ph)]^{2+}$ (1) and $[L(CO)_2Mo{\equiv}C\text{-}Ph)]^{+}$ (2) complexes.

Table 1. Bond lengths (Å) and bond angles (◦) of complex (1)

Bond	length (Å)	Bond	Angles (◦)
Mo36-N16	2.077	N16-Mo36-N17	87.1
Mo36-N17	2.077	N16-Mo36-N18	87.6
Mo36-N18	2.287	N16-Mo36-C19	104.2
Mo36-C19	1.853	N16-Mo36-C20	89.4
Mo36-C20	2.198	N16-Mo36-C21	170.7
Mo36-C21	2.198	N17-Mo36-N18	87.6
C19-C24	1.398	N17-Mo36-C19	104.2
C20-O23	1.133	N17-Mo36-C20	170.7
N3-N18	1.369	N17-Mo36-C21	89.3
N7-N16	1.378	N18-Mo36-C19	163.5
N11-N17	1.378	N18-Mo36-C20	83.6
N3-C4	1.352	N18-Mo36-C21	83.6
N7-C8	1.337	C19-Mo36-C20	85.0
N11-C12	1.337	C19-Mo36-C21	85.0
N16-C10	1.370	C20-Mo36-C21	92.9
N17-C14	1.370	H1-B2-N3	111.6
N18-C5	1.347	H1-B2-N7	109.8
B2-N3	1.532	H1-B2-N11	109.8
B2-N7	1.567	N3-B2-N7	109.3
B2-N11	1.567	N3-B2-N11	109.3
B2-H1	1.192	N7-B2-N11	106.8
C4-C6	1.388	C24-C19-Mo36	172.9

Table 2. Bond lengths (Å) and bond angles (◦) of complex (2)

Bond	length (Å)	Bond	Angles (◦)
Mo26-N12	2.145	N12-Mo26-N14	88.6
Mo26-N14	2.321	N12-M26-O25	89.3
Mo26-O25	1.975	N12-Mo26-C27	84.1
Mo26-C27	2.146	N12-Mo26-C28	173.6
Mo26-C28	2.134	N12-Mo26-C31	102.7
Mo26-C31	1.827	N14-Mo26-O25	90.5
C31-C32	1.420	N14-Mo26-C27	83.6
C27-O30	1.139	N14-Mo26-C28	85.0
C28-O29	1.140	N14-Mo26-C31	164.1
N11-N12	1.371	O25-Mo26-C27	171.3
N13-N14	1.362	O25-Mo26-C28	90.2
O25-C16	1.314	O25-Mo26-C31	100.6
C15-C16	1.442	C27-Mo26-C28	95.6
C16-C18	1.430	C27-Mo26-C31	86.5
N11-C6	1.342	C28-Mo26-C31	83.7
N12-C8	1.354	H1-B10-N11	105.7
N13-C2	1.348	H1-B10-N13	107.0
N14-C4	1.346	H1-B10-C15	109.5
B10-N11	1.572	N11-B10-N13	109.5
B10-N13	1.552	N11-B10-C15	112.6
B10-C15	1.630	N13-B10-C15	112.1
B10-H1	1.202	C32-C31-Mo26	171.0

As can be seen from Table 1 and Table 2, Mo36-N18 for the complex (1) and Mo26-N14 bonds for the complex (2) are longer from the other Mo-N bonds. The lengths of Mo36-N18 and Mo26-N14 bonds are 2.287 and 2.321 Å, respectively. These bonds contain the carbyne ligand in the trans position. The Mo-C(carbyne) lengths are 1.853 and 1.827 Å in the complex (1) and complex (2), respectively. This result indicates that Mo-C(carbyne) binding is stronger and carbyne carbon makes stronger back bonding. This result is consistent with that of many other carbyne complexes. In many other carbyne complexes, the length of M-C(carbyne) is given between 1.765-1.878 A° [21]. The stronger Mo-C(carbyne) bond caused weakening and elongation of the bonds in the trans position. The other bond lengths calculated for the complexes are consistent with the expected values and bond degrees.

C24-C19-Mo36 bond angle is calculated as 172.9° for complex (1) and C32-C31-Mo26 bond angle is obtained as 171.0° for complex (2). These M-C-R bond angles are consistent with similar carbyne complexes [21]. it is seen from these results that the carbyne carbon environmental geometry is near linear in the complex (1) and (2). As seen from the bond angles, the cis angles are about 90 degrees and the trans angles are about 180 degrees around the central metal atom. Therefore, central molybdenum environmental geometry is distorted octahedral. However, the angles N16-Mo36-C19 and N17-Mo36-C19 have deviated considerably from 90 degrees due to the steric and chelate effect. Boron atom environmental geometry in Tp ligand is distorted tetrahedral. The boron environment angles in the Tp ligand are expected to be 109.5 degrees. The calculated angles in boron environment are almost 109.5 degrees. Similar bonding angles have been obtained experimentally in similar carbyne complexes [13].

3.2. IR spectrum and labeling of peaks

IR spectrums of complex (1) and complex (2) were calculated at B3LYP/LANL2DZ/6-31G(d) level. The calculated IR spectrums are given in Fig. 3 with peak numbers.

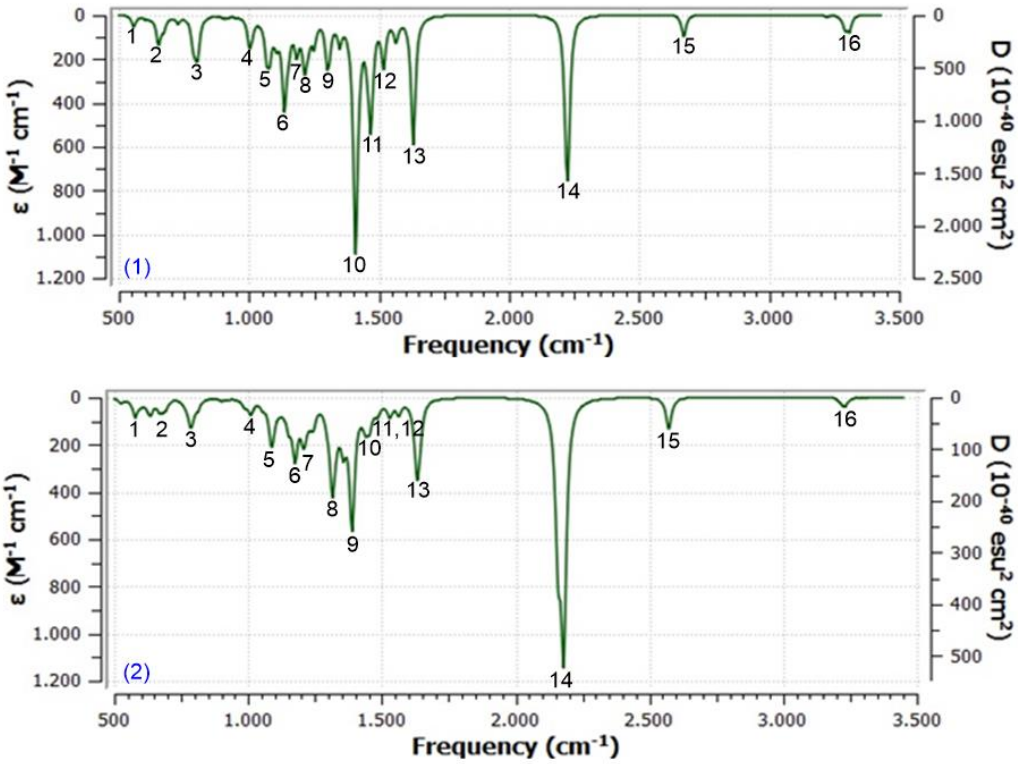

Figure 3. Calculated IR spectrum of complex (1) and complex (2).

Peak number, vibration mode number, frequencies and assignment of peaks given in Fig. 3 are given in Table 3 and Table 4. The frequencies in the tables are harmonic frequencies. No scale factor was found in the literature for the calculation level. Peak assignments were performed with vibrational energy distribution analysis (VEDA) program [22].

Table 3. Assignment of the peaks observed in the IR spectrum of the complex (1)

Peak No	Mod No	Frequency (cm^{-1})	Assignment
1	34	556.6	B (C-C-Mo), T (C-C-C-C)
2	41	651.6	S (Mo-C), B (C-C-C),
3	51	803.5	T (H-C-C-N), T (H-C-C-C)
4	65	1000.7	B (C-C-C)
5	71	1068.0	B (C-N-N)
6	77	1135.8	S (C-N)
7	81	1183.5	S (N-N)
8	84	1213.7	B (H-C-C)
9	88	1300.8	S (C-N)
10	93	1409.5	S (C-C)
11	98	1467.9	S (C-C), B (C-N-N)
12	101	1517.4	S (C-C), B (H-C-C)
13	106	1631.7	S (C-C)
14	108	2226.5	S (C-O)
15	109	2672.1	S (B-H)
16	120	3295.1	S (C-H)

B: Bending, T: Torsion, S: Stretching

Table 4. Assignment of the peaks observed in the IR spectrum of the complex (2)

Peak No	Mod No	Frequency (cm^{-1})	Assignment
1	38	577.9	B (C-C-C), T (C-N-N-C)
2	43	635.1	B (O-C-C), B (C-C-C)
3	45	667.6	S (Mo-C), B (C-C-C)
4	70	1008.4	B (C-C-C)
5	77	1086.9	S (C-C), B (N-N-C), B (H-C-C)
6	85	1175.8	S (C-C), S (C-B), B (H-C-C), B (H-B-C)
7	88	1206.3	S (N-C), S (N-N)
8	94	1315.4	S (C-O) phenoxy
9	100	1388.9	S (C-C)
10	103	1454.3	B (H-C-C)
11	108	1529.5	S (C-C), B (H-C-C)
12	110	1563.7	S (C-C), B (H-C-C)
13	113	1631.7	S (C-C), B (H-C-C)
14	116	2179.8	S (C-O)
15	117	2572.6	S (B-H)
16	125	3230.6	S (C-H)

B: Bending, T: Torsion, S: Stretching

As shown in Table 3 and Table 4, bending, torsion and Mo-C(carbyne) stretching vibrations are observed in the 500-1000 cm^{-1} region. Bending and torsion vibrations have no important function in determining the structure. However, the peak of Mo-C(carbyne) stretching vibrations was calculated in this region. The frequencies of 651.6 cm^{-1} for complex (1) and 667.6 cm^{-1} for complex (2) belong to the Mo-C(carbyne) bond stretching vibration. It is known that the vibration frequencies $(\bar{\nu})$ are directly proportional to the square root of the bond force constant (k) and inversely proportional to the square root of reduced masses (μ) of the connected atoms according to the Eq. 11.

$$\bar{\nu} = \frac{1}{2\pi c}\sqrt{\frac{k}{\mu}} \qquad (11)$$

For Mo-C bonds, in general, the Mo-C stretching frequencies are expected to be small since the force constant is small and the reduced mass is large. Therefore, Mo-C stretching vibrations are observed at low frequency.

Numerous peaks emerged in the region of 1000-1650 cm^{-1}. This is the region where single and double bond stretching vibrations are observed. In this region, peaks of C-C, C=C, N-N, C-N, C=N, B-N, C-O(phenoxy) bond stretching vibrations and some bending vibrations were calculated.

Peaks of C-O stretching for both complexes are very prominent. The peaks 14 for the complex (1) and (2) belong to C-O stretching vibrations. For both complexes, these frequencies are in the carbonyl stretching region. Another prominent peak in the IR spectrum of complexes is related to B-H stretching. B-H stretching frequencies were calculated at 2672.1 cm^{-1} in the complex (1) and 2572.6 cm^{-1} in the complex (2). C-H, N-H, O-H vibrations are observed around 3000 cm^{-1}. Although these bonds are single bonds, they are observed at high frequency because the reduced mass is small. The smaller the reduced mass according to eq. (11), the greater the frequency of the vibration.

3.3. UV-VIS spectrum and main band assignment

UV-VIS spectrums of the complexes were calculated at TD-B3LYP/LANL2DZ/6-31G(d) level in gas phase and given in Fig. 4. The bands in the UV-VIS spectrum of the molecules arise from allowed electronic transitions. The allowed electronic transitions have a molar absorption coefficient greater than 1000 L/mol.cm. Electronic transitions with large molar absorption coefficients are shown in Fig. 4 with band number.

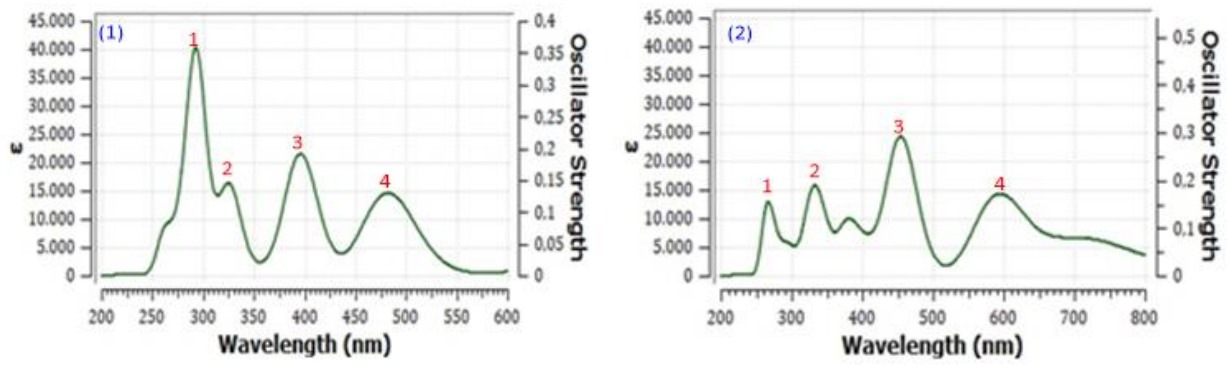

Figure 4. Calculated UV-VIS spectrums of the complex (1) and (2)

As shown in Fig. 4, there are four bands in the UV-VIS spectrum of the both complexes. Main band is shown with number 1 for complex (1) and number 3 for complex (2). Here, the electronic transitions forming the main bands will be analyzed. Table 5 shows the wavelengths of the main bands, the electronic transitions forming the main bands and the wave function coefficients of the electronic transitions for each excitation.

Table 5. Wavelengths of the main bands in the UV-VIS spectra of the studied complexes, electronic transitions forming the main bands and wave function coefficients

Complex	Wavelength (nm)	Transitions	Wave function coefficient
(1)	294.1	HOMO-13 → LUMO	0.199
		HOMO-4 → LUMO+2	0.145
		HOMO-2 → LUMO+2	0.576
		HOMO-1 → LUMO+1	0.238
(2)	454.9	HOMO-9 → LUMO	0.163
		HOMO-8 → LUMO	0.621
		HOMO-6 → LUMO	-0.124
		HOMO-1 → LUMO	0.173
		HOMO → LUMO	0.117

When the wave function coefficients of the electronic transitions which form the main band (294.1 nm) of complex (1) are examined, it is seen that the wave function coefficient of HOMO-2 → LUMO+2 electronic transition is the highest. This finding indicates that the highest contribution to the formation of the main band of complex (1) is due to the electronic transition of HOMO-2 → LUMO+2. Likewise, it can be said that the main band (454.9 nm) of complex (2) is mainly caused by HOMO-8→LUMO transition. The characters of these orbitals can be determined from wave function coefficients or contour diagrams. The contour diagrams of HOMO-2, LUMO+2 for complex (1) and HOMO-8 and LUMO for complex (2) are given in Figure 5.

For complex (1), it can be said that HOMO-2 is a π molecular orbital consisting of the overlap of molybdenum d orbital and carbyne carbon p orbital in two regions. LUMO+2 is a π* antibonding molecular orbital formed by the difference between molybdenum d orbital and carbyne carbon p orbital.

The HOMO-2 → LUMO+2 transition is then a π→π* transition. HOMO-8 of complex (2) represents π molecular orbital formed by the overlap of the p orbitals of the carbon atoms in the pyrazole ring. LUMO indicates π* orbitals consisting of central molybdenum d orbitals and phenoxy oxygen p orbitals [23]. Therefore, this electronic transition can be considered as a ligand-to-metal charge transfer transition (LMCT). The same results are obtained when the molecular orbital coefficients are examined.

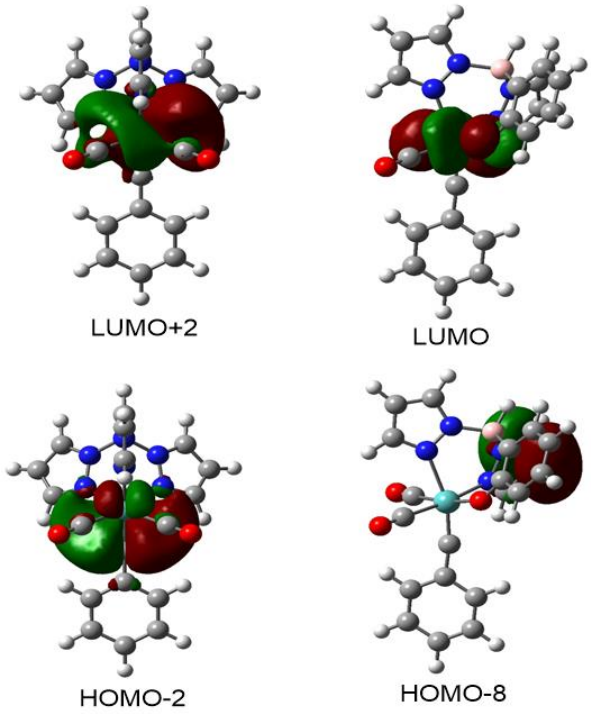

Figure 5. Contour diagrams of HOMO-2, LUMO+2 for complex (1) and HOMO-8 and LUMO for complex (2)

3.4. ^{1}H-NMR and ^{13}C-NMR spectrums and assignment of peaks

^{1}H-NMR and ^{13}C-NMR spectrums of the complexes were computed with Gauge-Independent Atomic Orbital (GIAO) method at the level of B3LYP/LANL2DZ/6-31G(d). Tetramethyl silane (TMS) was taken as reference to determine chemical shifts. Chemical shift of carbon and hydrogen atoms for TMS in the same level were calculated as 193.0 and 32.4 ppm, respectively. ^{1}H-NMR and ^{13}C-NMR spectrums of the complexes are given in Fig. 6 and Fig. 7. ^{1}H and ^{13}C-NMR chemical shift values are given in Table 6.

As can be seen from Figure 6, Figure 7 and Table 6, there are seven peaks in the ^{1}H-NMR spectrums of both complexes. Some protons have the same chemical shift value. This result indicates that some hydrogens are equivalent. The chemical shift value of hydrogen bound to the boron atom was calculated as 4.65 ppm for complex (1) and 4.47 ppm for complex (2). The chemical shift values of the hydrogens bonded carbon atoms vary between 5.9-8.4 ppm. This can be explained by the fact that the hybridization types of boron and carbon atoms are different [24]. Carbon atoms have sp^2 hybridization and boron atom sp^3 hybridization. S-characters of the hybrid orbitals in the boron atom are about 25%, whereas the s-characters of the hybrid orbitals in the carbon atom are about 33%.

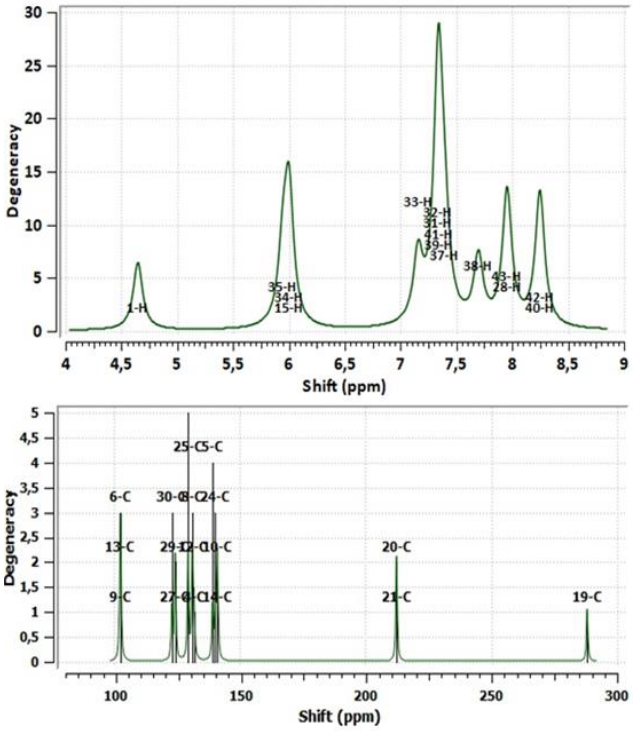

Figure 6. ^{1}H-NMR and ^{13}C-NMR spectra for $[Tp(CO)_2Mo{\equiv}C\text{-}Ph)]^{2+}$ complex calculated at B3LYP/LANL2DZ/6-31G(d) level by GIAO method

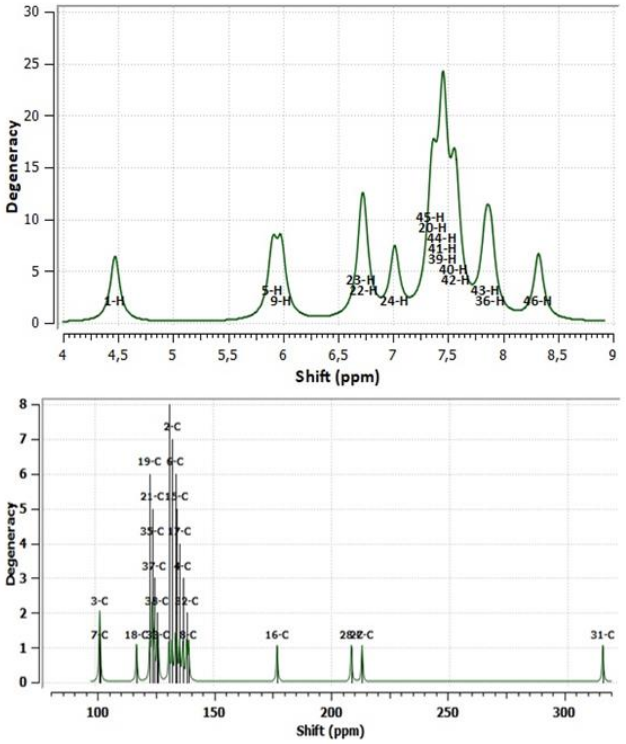

Figure 7. ^{1}H-NMR and ^{13}C-NMR spectra for $[L(CO)_2Mo{\equiv}C\text{-}Ph)]^{+}$ complex calculated at B3LYP/LANL2DZ/6-31G(d) level by GIAO method

Table 6. ^{1}H and ^{13}C-NMR chemical shift values (ppm) of the studied complexes

Complex (1)		**Complex (2)**	
^{1}H-NMR assignment	δ(ppm)	^{1}H-NMR assignment	δ(ppm)
1H	4.65	1H	4.47
15H,34H,35H	5.95-6.00	5H,9H	5.91-5.98
33H	7.16	22H,23H	6.71-6.74
31H,32H,37H,39H,41H	7.34-7.39	24H	7.02
38H	7.70	20H,39H,40H,41H,42H,44H,45H	7.35-7.58
28H,43H	7.95	36H,43H	7.84-7.89
40H,42H	8.25	46H	8.32
^{13}C-NMR assignment	δ(ppm)	^{13}C-NMR assignment	δ(ppm)
6C,9C,13C	102.7	3C,7C	102.2
27C,29C,30C	123.1-124.4	18C	117.8
25C,26C	129.6	19C,21C,33C,35C,37C,38C	123.4-126.9
4C,8C,12C	131.2-131.9	2C,4C,6C,8C,15C,17C,32C,34C,	131.5-139.8
5C,10C,14C,24C	139.3-141.2	16C	177.2
20C,21C	212.4	28C	208.6
19C	288.1	27C	213.1
		31C	314.9

As the s-character of the hybrid orbitals decreases, the nuclei are more shielded by electrons. Highly shielded nuclei are observed at low chemical shift value. Therefore, the chemical shift of the hydrogen bound to the boron atom is lower. The slightly different chemical shift values of the hydrogens bound to carbon atoms are related to the distance of the carbon atoms to the electronegative atom. The chemical shift values of the hydrogens attached to carbons close to the electronegative atom such as nitrogen and oxygen are slightly higher. Because the nuclei of the carbons adjacent to the atom with high electronegativity are less shielded. The less shielded core is observed at high ppm.

When the ^{13}C-NMR spectra and chemical shift values of the complexes are examined, it is seen that the chemical shift of the carbyne carbon is higher than the others. 19C = 288.1 ppm for complex (1) and 31C = 314.9 ppm for complex (2). In general, the chemical shift of carbon atoms with M≡C binding is reported to be between 235-401 ppm [25]. The chemical shift values calculated in this study are consistent with these results. The calculated carbonyl carbon chemical shift values are also around 210 ppm. Experimentally, ^{13}C-chemical shift values for M-CO bonded carbonyl compounds are generally in the range of 177-275 ppm [25]. The values calculated in this study are in agreement with this range. 16C chemical shift (177.2 ppm) in complex (2) is also different. This value belongs to the carbon to which the phenoxy group oxygen is attached. The high electronegativity of oxygen leads to a reduction in electron density on 16C and less shielding of the nucleus. The less shielded core has a high chemical shift value. As can be seen from Table 6, the chemical shift of other carbons is between 100-140 ppm. These values vary according to the chemical environment of carbon atoms. Carbons with electronegative atoms around have a higher chemical shift value.

3.5. Charge distribution

In order to estimate the electronic structures of the complexes, charges of some atoms, electrostatic potential maps of the complexes, molecular orbital energy diagrams and frontier orbital contour diagrams were calculated. The charges of the atoms in the complexes were calculated according to Mulliken method. Mulliken charges of some atoms are given in Table 7.

Table 7. Mulliken charges of some atoms in the complexes

Complex (1)		Complex (2)	
Atom	Charge	Atom	Charge
2B	0.484	10B	0.344
16N	-0.417	12N	-0.385
17N	-0.417	14N	-0.318
18N	-0.339	25O	-0.556
19C	-0.161	26Mo	0.843
20C	0.298	27C	0.280
21C	0.298	28C	0.254
36Mo	0.946	31C	-0.184

It was considered that central molybdenum is +3 charged, hydridotris(pyrazolyl)borate (Tp) ligand is -1 charged and hydrido-2-phenoxybis(pyrazolyl)borate (L) is -2 charged in the computational design. In this case, the total charge of complex (1) is +2 and the total charge of complex (2) is +1. As shown in Table 7, positive formal charges were calculated for boron atoms (2B, 10B) in the Tp and L ligands, carbonyl carbon (20C, 21C, 27C, 28C) and central molybdenum atoms. Negative formal charges were obtained for donor nitrogen atoms (16N, 17N, 18N,12N, 14N) phenoxy group oxygen atom (25O) and carbyne carbons (19C, 31C). It is seen that central molybdenum atom reduces the positive charge in complex formation. The molybdenum atom, which was considered to be +3 charged in the isolated state, had a charge of +0.946 in complex (1) and +0.843 in complex (2). This result indicates that molybdenum receives electrons from the ligands in complex formation. In the complexes, the formal charges of carbyne carbons appear to be very close to zero. This is suitable for metal-carbyne back bonding. Carbyne carbon gives electrons in sp hybrid orbitals to metal and positively charged. However, the low-energy p orbitals receive electrons from the metal and negatively charged. The similar $Cl(CO)_4Cr{\equiv}C\text{-}Ph$ complex were studied by Dao *at al*. Electronic charges were obtained from X-ray and neutron diffraction methods. It is seen that there is a partial negative charge on the carbyne carbon atom [26].

3.6. Molecular electrostatic potential (MEP) maps

MEP maps were calculated to determine the regions of the complexes suitable for nucleophilic and electrophilic attacks. The colors in these maps range from red to blue. In the MEP maps, the red zone electron density is the highest and the blue zone electron density is the lowest. Thus, the molecule can attack the nucleophiles from the red region and the electrophiles from the blue region. MEP maps of carbyne complex ions were calculated at B3LYP/LANL2DZ/6-31G(d) level and given in Figure 8.

As shown in Fig. 8, the MEP map of complex (1) is darker-blue. The darker-blue indicates that the electron density is low and the electrophilicity of the complex is high. According to this assessment, complex (1) is more electrophilic than complex (2). This is also consistent with the charges of the complexes. Since both complexes are positively charged, there are no red regions with high electron density in the MEP maps.

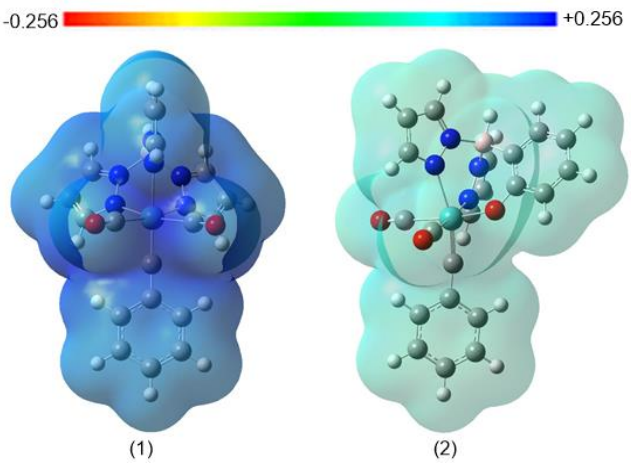

Figure 8. MEP maps of complex (1) and complex (2)

3.7 Molecular orbital energy diagrams and frontier orbital contour diagrams

The diagrams obtained by ordering the molecular orbitals according to their increasing energy are called molecular orbital energy diagram (MOED). The energies of the highest occupied molecular orbital (E_{HOMO}) and the lowest unoccupied molecular orbital (E_{LUMO}) and contour diagrams of frontier orbitals are generally used to estimate the electronic properties. Molecular orbital energy diagrams of the complexes between HOMO-4 and LUMO+4 and contour diagrams of HOMO, LUMO are given in Figure 9.

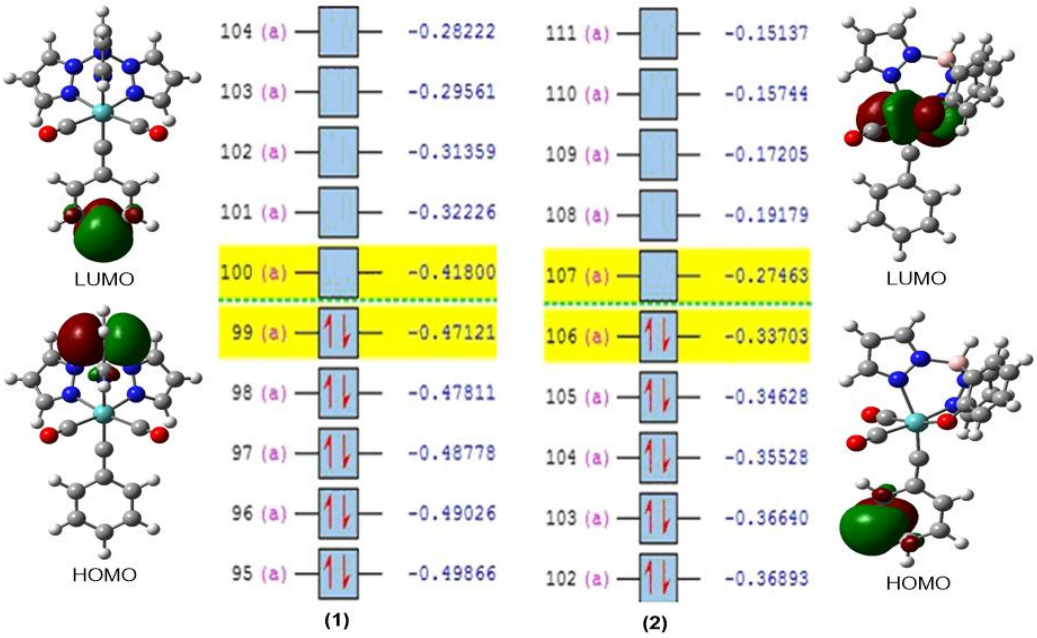

Figure 9. Contour diagrams of the frontier orbitals and MOED for complexes (1) and (2).

Table 8. Some molecular properties calculated for B3LYP/LANL2DZ/6-31G(d) level for complex (1) and complex (2)

Descriptor	(Unit)	Complex (1)	Complex (2)
E_{HOMO}	eV	-12.8188	-9.1686
E_{LUMO}	eV	-11.3713	-7.4710
I	eV	12.8188	9.1686
A	eV	11.3713	7.4710
ΔE	eV	1.4475	1.6975
η	eV	0.7238	0.8488
σ	eV^{-1}	1.3817	1.1782
χ	eV	12.0950	8.3198
CP	eV	-12.0950	-8.3198
ω	eV	101.0616	40.7763
μ	D	3.5757	1.9049
α	$Å^3$	345.6023	390.1813

As can be seen from the molecular orbital energy diagram of the complexes, E_{HOMO} = -0.4712 and E_{LUMO} = -0.4180 for complex (1), E_{HOMO} = -0.3370 and E_{LUMO} = -0.2746 for complex (2). Here the energies are in the Hartree unit. 1 Hartree = 27.2116 eV. For complex (1), HOMO is concentrated on the boron atom, LUMO is concentrated on the phenyl ring. On the other hand, for complex (2), HOMO is concentrated on the phenyl ring and LUMO is concentrated on the central molybdenum atom. HOMO is the orbital where the first electron will be removed and LUMO is the first electron to enter.

3.8. Some electronic structure descriptors

Some molecular structure descriptors such as ionization energy (I), electron affinity (A), LUMO-HOMO energy gap (ΔE), chemical hardness (η), chemical softness (σ), Mulliken electronegativity (χ), chemical potential (CP), electrophilicity index (ω), static dipole moment (μ) and average linear polarizability (α) were calculated for predicting the molecular properties of the complexes. HOMO and LUMO energies were taken from the molecular orbital energy diagrams (MOED). The electronic structure descriptors calculated from eq. (1)-(10) are given in Table 8.

As seen from eq. (1) and eq. (2), HOMO and LUMO energies is connected with ionization energy (I) and electron affinity (A) according to the Koopmans theorem [27]. It is seen from Table 8 that the HOMO energy of complex (1) is lower than that of complex (2). The lower ionization energy of complex (1) is higher than that of complex (2) since the low HOMO energy will cause higher ionization energy. LUMO energy is also associated with electron affinity. Again, the LUMO energy of complex (1) is low and the electron affinity of complex (1) is higher than that of complex (2).

It is seen from the equation (3) - (7) that the energy gap is associated with hardness, softness, electronegativity and chemical potential. The species with a large energy gap are harder and the smaller ones are softer. Since the ΔE value of complex (1) is higher than that of complex (2), complex (1) is harder than complex (2) [28].

Mulliken electronegativity is defined as the arithmetic mean of ionization energy (I) and electron affinity (A).

The higher the I and A values, the higher the χ value and the lower the CP. As shown in Table 8, since the I and A values of complex (1) are higher than those of complex (2), χ value is higher and CP value is lower.

The higher the electrophilicity index, the higher the electrophilicity. An electrophile interacts more strongly with a nucleophile and there is more electron flow in this interaction. This electron flux reduces the energy more. As shown in Table 8, the ω value of complex (1) is higher than that of complex (2). Therefore, complex (1) is more electrophile. This result is consistent with the results obtained from MEP maps.

Dipole moment is a measure of the polarity of compounds. Molecules with a dipole moment greater than zero are called polar molecules. In this sense, the complexes studied are both polar. Polarizability can be defined as the softness of the electron cloud of the molecule. According to the data in Table 8, the polarizability (α) of complex (2) is higher than complex (1). It is stated that substances whose polarizability (α) and hyperpolarizability (β) are higher than those of urea can be used in production of nonlinear optical materials [29]. The polarizabilities of both complexes are higher than that of urea (α=5.0708 $Å^3$, β=5.30x10^{-28} cm^5/esu for urea). Complexes can be used to make nonlinear optical materials according to their polarizability values.

3.9. Thermochemistry of the complexes

It has already been stated that due to the thermal instability of most alkylidine complexes, it has been studied in a limited manner [13]. In this paper, thermal stability of the hypothetical complex (1) and complex (2) were investigated computationally. Complex (1) and complex (2) were optimized in the gas phase at a pressure of 1.00 atm and temperatures of 200, 298.15 and 400 K at the level of B3LYP/LANL2DZ/6-31G(d). Imaginary frequency was not obtained as a result of the optimization. This finding indicates that the complexes are in the ground state with minimum energy. Thermochemical parameters which are total energy (E), enthalpy (H), heat capacity (C_v) and entropy (S) obtained at 200, 298.15 and 400 K temperatures for the complexes are given in Table 9.

Table 9. Thermochemical parameters at various temperatures for complex (1) and complex (2)

Complex	Thermochemical parameters	Temperature (K)		
		200	298.15	400
Complex (1)	E[a]	-1265.4433	-1265.4307	-1265.4132
	H[a]	-1265.4426	-1265.4297	-1265.4119
	C_v[b]	67.354	94.164	120.152
	S[b]	143.455	176.124	208.105
Complex (2)	E[a]	-1346.3984	-1346.3850	-1346.3664
	H[a]	-1346.3978	-1346.3841	-1346.3652
	C_v[b]	70.935	100.218	128.270
	S[b]	148.319	182.908	216.924

[a] Hartree, [b] cal/molK

As shown in Table 9, thermochemical parameters of complexes increase as the temperature increases. This result indicates that the stability of the complexes decreases with increasing temperature. The following equations were obtained for the relationship between thermochemical parameters and temperature.

For complex (1)

$$E = 2.13158x10^{-7}T^2 + 2.24551x10^{-5}T - 1.26546x10^{3} \qquad R^2 = 0.999$$

$$H = 2.13172x10^{-7}T^2 + 2.56169x10^{-5}T - 1.26546x10^{3} \qquad R^2 = 0.999$$

$$C_v = -8.99689\,x10^{-5}T^2 + 3.17971T + 7.35848 \qquad R^2 = 1.000$$

$$S = -9.422335\,x10^{-5}T^2 + 3.79790\,x10^{-1}T + 7.12663\,x10^{1} \qquad R^2 = 1.000$$

For complex (2)

$$E = 2.31241x10^{-7}T^2 + 2.11903x10^{-5}T - 1.34641x10^{3} \qquad R^2 = 1.000$$

$$H = 2.31255x10^{-7}T^2 + 2.43522x10^{-5}T - 1.34641x10^{3} \qquad R^2 = 1.000$$

$$C_v = -1.14624\,x10^{-4}\,T^2 + 3.55449\,x10^{-1}\,T + 4.43007 \qquad R^2 = 1.000$$

$$S = -9.21412x10^{-5}\,T^2 + 3.98310x10^{-1}\,T + 7.23427x10^{1} \qquad R^2 = 1.000$$

As shown in these equations, R^2 values are almost equal to one. Thermochemical parameters can then be calculated for a given temperature using these equations. At the same time, the temperature required to break a metal-carbyne triple bond can be calculated. The bond dissociation energy of M≡CH triple bond is given as 523, 477, 607, 423 and 418 kJ/mol for La, V, Nb, Fe and Co, respectively [21]. When these values are averaged, the average bond dissociation energies of M≡C triple bonds are found to be 490 kJ/mol. Carbyne complexes are reported to be stable at room temperature. Thus, when the energy at 298.15 K of the carbyne complex is increased about 490 kJ/mol, the metal-carbyne triple bond can be broken. Since 1 Hartree is equal to $4.3597482x10^{-18}$ Joule [30], 490 kJ/mol is equal to 0.186631 Hartree. When 0.186631 Hartree is added to total energies of complex (1) and complex (2) at 298.15 K and replaced in the total energy equation, the following equations are obtained.

For complex (1) $$2.13158\,x10^{-7}\,T^2 + 2.24551\,x10^{-5}\,T - 2.159721\,x10^{-1} = 0$$

For complex (2) $$2.31241\,x10^{-7}\,T^2 + 2.11903\,x10^{-5}\,T - 2.115860\,x10^{-1} = 0$$

When these equations are solved for temperature, the M≡C bond dissociation temperatures of complex (1) and complex (2) are found to be 955 and 912 K. These results show that the hypothetical carbyne complexes designed can be stable at high temperatures. In addition, the bond dissociation energy of complex (1) is higher than that of complex (2).

4. Conclusion

Structural, electronic, molecular and thermochemical properties of hypothetical $[Tp(CO)_2Mo{\equiv}C\text{-}Ph)]^{2+}$ **(1)** and $[L(CO)_2Mo{\equiv}C\text{-}Ph)]^{+}$ **(2)** carbyne complexes were investigated by B3LYP/ LANL2DZ/6-31G(d) level. Bond lengths, bond angles, IR, UV-Vis and ^{1}H-NMR, ^{13}C-NMR spectrums were calculated to predict the complex structures. Charges of some atoms, MEP maps, molecular orbital energy diagrams and frontier orbital contour diagrams were calculated to estimate the electronic structures of the complexes. Some molecular structure descriptors were calculated for predicting the molecular properties. In order to predict the thermochemical stability of the complexes, total energy (E), enthalpy (H), heat capacity (C_v) and entropy (S) were calculated at 200, 298.15 and 400 K temperatures. It is found that hypothetical carbyne complexes designed in this study can be stable at high temperatures.

Acknowledgments

The authors are grateful for their support to the Sivas Cumhuriyet University, Scientific Research Unit (Project No: F-580).

Conflict of interest

The authors state that there is no conflict of interests.

References

[1] Fischer E. O., Kreis G., Kreiter C. G., Müller J., Huttner G., Lorenz H., trans-Halogeno [alkyl(aryl)carbyne] tetracarbonyl Complexes of Chromium, Molybdenum and Tungsten, A New Class of Compounds Having a Transition Metal-Carbon Triple Bond, *Angewandte Chemie International Edition in English*, 12(7) (1973) 564-565.

[2] Wu X., Daniliuc C.G., Hrib C.G., Tamm M., Phosphoraneiminato tungsten alkylidyne complexes as highly efficient alkyne metathesis catalysts, *Journal of Organometallic Chemistry*, 696(25) (2011) 4147-4151.

[3] Lysenko S., Daniliuc C. G., Jones P. G., Tamm M., Tungsten alkylidyne complexes with ancillary imidazolin-2-iminato and imidazolidin-2-iminato ligands and their use in catalytic alkyne metathesis, *Journal of Organometallic Chemistry*, 744 (2013) 7-14.

[4] Fey N., Orpen A. G., Harvey J. N., Building ligand knowledge bases for organometallic chemistry: Computational description of phosphorus (III)-donor ligands and the metal–phosphorus bond, *Coordination Chemistry Reviews*, 253(5-6) (2009) 704-722.

[5] Snelders D. J., Van Koten G., Klein Gebbink R. J., Steric, electronic, and secondary effects on the coordination chemistry of ionic phosphine ligands and the catalytic behavior of their metal complexes, *Chemistry–A European Journal*, 17(1) (2011) 42-57.

[6] Díez-González S., Nolan S. P., Stereo electronic parameters associated with N-heterocyclic carbene (NHC) ligands: a quest for understanding, *Coordination Chemistry Reviews*, 251(5-6) (2007) 874-883.

[7] Peris E., Smart N-heterocyclic carbene ligands in catalysis, *Chemical Reviews*, 118(19) (2017) 9988-10031.

[8] Kim H. P., Angelici R. J., Transition metal complexes with terminal carbyne ligands, *In Advances In Organometallic Chemistry*, 27 (1987) 51-111.

[9] Hart I. J., Hill A. F., Stone F. G. A., Synthesis of alkynylmethylidyne molybdenum and-tungsten complexes and their reactions with octacarbonyldicobalt and hexacarbonylbis (g-cyclopentadienyl) dimolybdenum, *J. Chem. Soc. Dalton Trans*, (1989) 2261-2267.

[10] McDermott G. A., Dorries A. M., Mayr A., Synthesis of carbyne complexes of chromium, molybdenum, and tungsten by formal oxide abstraction from acyl ligands, *Organometallics*, 6(5) (1987) 925-931.

[11] Dossett S. J., Hill A. F., Jeffery J. C., Marken F., Sherwood P., Stone F. G. A., Chemistry of polynuclear metal complexes with bridging carbene or carbyne ligands. Part 79. Synthesis and reactions of the alkylidynemetal complexes [M([triple bond, length half m-dash]CR)$(CO)_2$(η-C_5H_5)] (R=C_6H_3, Me 2-2, 6, M=Cr, Mo, or W; R=C_6H_4Me-2, C_6H_4OMe-2, or C_6H_4NMe2-4, M= MO); crystal structure of the compound [MoFe(μ-CC_6H_3 Me2-2,6)$(CO)_5$(η-C_5H_5)], *Journal of the Chemical Society Dalton Transactions*, (9) (1988) 2453-2465.

[12] Fernández J.R., Stone F.G.A., Chemistry of polynuclear metal complexes with bridging carbene or carbyne ligands. Part 83. Molybdenum and tungsten complexes containing the alkylidyne group C{η^6-C_6H_4(OMe-2)Cr$(CO)_3$}, *Journal of the Chemical Society Dalton Transactions*, (12) (1988) 3035-3040.

[13] Hazra D., Sinha-Mahapatra D. K., Puranik V. G., Sarkar A., Synthesis and structure of novel, air-stable carbyne complexes of tungsten, *Journal of Organometallic Chemistry*, 671(1-2) (2003) 52-57.

[14] Dennington R. D., Keith T. A., Millam C. M., GaussView 5.0 Wallingford. In CT, (2009).

[15] Frisch M. J., Trucks G. W., Schlegel H. B., Scuseria G. E., Robb M. A., Cheeseman, J. R., Nakatsuji H., Gaussian 09, (Revision A. 1, Inc., Wallingford CT) (2009).

[16] Becke A. D., Density - functional thermochemistry. I. The effect of the exchange-only gradient correction, *The Journal of Chemical physics*, 96(3) (1992) 2155-2160.

[17] Lee C., Yang W., Parr R. G., Development of the Colle-Salvetti correlation-energy formula into a functional of the electron density, *Physical Review B.*, 37(2) (1988) 785.

[18] Karakaş D., Kariper S.E., Theoretical investigation on the vibrational and electronic spectra of three isomeric forms of dicobalt octacarbonyl, *Journal of Molecular Structure*, 1062 (2014) 77-81.

[19] Gövdeli N., Karakaş D., Quantum chemical studies on hypothetical Fischer type $Mo(CO)_5$[C(OEt)Me] and $Mo(CO)_5$[C(OMe)Et] carbene complexes, *Journal of Molecular Structure*, 1163 (2018) 94-102.

[20] Erkan S., Karakaş D., Computational investigation of structural, nonlinear optical and anti-tumor properties of dinuclear metal carbonyls bridged by pyridyl ligands with alkyne unit, *Journal of Molecular Structure*, 1199 (2020) 127054.

[21] Mayr A., Hoffmeister H., Recent advances in the chemistry of metal-carbon triple bonds, *In Advances In Organometallic Chemistry*, 32 (1991) 227-324.

[22] Jamróz M. H., Vibrational energy distribution analysis (VEDA): scopes and limitations, *Spectrochimica Acta Part A: Molecular and Biomolecular Spectroscopy*, 114 (2013) 220-230.

[23] Majumdar D., Das S., Thomas R., Ullah Z., Sreejith S.S., Das D., Shukla P., Bankura K., Mishra D., Syntheses, X-ray crystal structures of two new Zn(II)-dicyanamide complexes derived from H2vanen-type compartmental ligands: Investigation of thermal, photoluminescence, in vitro cytotoxic effect and DFT-TDDFT studies, *Inorganica Chimica Acta*, 492 (2019) 221-234

[24] Bowser J. R., Inorganic Chemistry, Brooks, Cole Publishing Company, (1993) 721-725

[25] Miessler G. L., Tarr D. A, Inorganic Chemistry, 2nd ed., New Jersey, Prentice Hall, (2003) 472-474.

[26] Spasojevic-de Bire A., Dao N. Q., Fischer E. O., Hansen N.K., trans-Chlorotetracarbonyl (phenylmethylidyne) chromium: experimental electron deformation density, *Inorganic Chemistry*, 32(23) (1993) 5354-5361.

[27] Pearson R. G., Absolute electronegativity and hardness: application to inorganic chemistry, *Inorganic Chemistry*, 27(4) (1988) 734-740.

[28] Majumdar D., Agrawal Y., Thomas Y., Ullah Z., Santra M. K., Das S., Pal T.K., Bankura K., Mishra D., Syntheses, characterizations, crystal structures, DFT/TD-DFT, luminescence behaviors and cytotoxic effect of bicompartmental Zn (II)-dicyanamide Schiff base coordination polymers: An approach to apoptosis, autophagy and necrosis type classical cell death, *Applied Organometallic Chemistry*, 34(1) (2020) 5269.

[29] Kose M., Hepokur C., Karakas D., McKee V., Kurtoglu M., Structural, computational and cytotoxic studies of square planar copper (II) complexes derived from dicyandiamide, *Polyhedron*, 117 (2016) 652-660.

[30] Cohen E. R., Taylor B. N., The 1986 adjustment of the fundamental physical constants, *Reviews of Modern Physics*, 59(4) (1987) 1121.